

REMOTE SENSING FOR MAPPING AND MODELING PRESENCE OF ARMYWORM  
INFESTATION ON MAIZE IN EJURA, GHANA

By

Thomas Bilintoh

A THESIS

Submitted to  
Michigan State University  
in partial fulfillment of the requirements  
for the degree of

Geography-Master of Science

2019

## **ABSTRACT**

### **REMOTE SENSING FOR MAPPING AND MODELING PRESENCE OF ARMYWORM INFESTATION ON MAIZE IN EJURA, GHANA**

By

Thomas Bilintoh

The African armyworm poses a significant threat to human food security in many regions. Detecting and monitoring the effects of this pest is, therefore, an activity that needs to be carried out with the utmost urgency. Field surveys in combination with remote sensing have the potential to play a pivotal role in understanding the distribution and effects of the African armyworm. However, finding remotely sensed data and reliable variables from field surveys to model and predict African armyworm distribution can be a daunting activity. Some of the challenges include: which vegetation index to use, how to manage cloud cover in satellite imagery and which spatial and temporal resolution to select. On the other hand, field surveys are not only subject to biased responses but a lack of recall power from the respondents. Despite these challenges, the onus falls on the research community to provide methods that can help address the uncertainties in these data sources for research on armyworm impacts on crops. This thesis consists of two coupled studies on armyworm infestation in Ejura, Ghana. The first is concerned with modeling the relationship between farmer-provided survey responses and vegetation quality as captured by satellite remote sensing. To assess the accuracy of field survey responses, the first study begins by hypothesizing that Enhanced Vegetation Index (EVI) has a positive correlation with armyworm infestation. This hypothesis was then tested through a logistic regression, where the dependent variable was farmers' declaration of presence or absence of armyworm infestation in 2017. Independent variables were principal components that measured slope and EVI from Landsat 8 for April, May, and July of 2017. Results from the logistic analysis revealed that there was no correlation between EVI, slope and armyworm infestation. Interestingly, a prediction model resulting from the logistic model

performed well by correctly predicting 11 out of 13 armyworm infestation cases. Nevertheless, the model could only predict one case of absence of armyworm infestation out of five cases. The second study contrast two vegetation index products obtained at very different spatial resolutions. I envisage possible applications of the second finding from the second study in addressing the issue of cloud cover in satellite-based remote sensing by resampling fine-scale Parrot Sequoia imagery to Landsat 8 (30 m resolution) imagery. Although a time lag of 4 days was present between Landsat 8 imagery and data obtained from Parrot Sequoia multispectral camera deployed on a UAV, a prediction accuracy of 0.67 was achieved. Developing a technique that could rescale Parrot Sequoia data to Landsat 8 imagery is a novel aspect of this work. Fishnet, which is a popular tool in ArcMap, was instrumental in the rescaling phase of this study. Mapping residuals from the EVI (Landsat 8) and EVI2 (rescaled Parrot Sequoia) image showed that the regression model developed predicted well in areas with high and homogenous vegetation as compared to areas with low and heterogeneous vegetation.

## **ACKNOWLEDGEMENTS**

I would like to say thank you to my wife for her unending support, love and patience throughout my graduate education at Michigan State University. To Professor Ashton Shortridge, I say I will forever be grateful. You have been instrumental not only to the successful completion of my graduate course but been a driving force that has stirred my consciousness in mentor and mentorship. Your kindness, patience and insightful way of inspiring me even when I felt this work had hit a 'dead end' is something I would always cherish. Dr. Raechel Portelli, thank you for being a part of this wonderful work. I am also grateful to you for connecting me with the remote sensing community and trusting in my capabilities even when we had just met for an ephemeral period. Many thanks to Professor Qi for stirring up my research senses in the field of remote sensing. Your class in Digital Image Processing and Analysis is what has metamorphosed into this work. I appreciate every single time you gave me out of your busy schedule. Above all I am most grateful to the MasterCard Foundation Scholars program for supporting me financially and emotionally throughout my graduate studies.

I dedicate this work to all the youth back on the African continent who dream of making a difference in the world someday.

## TABLE OF CONTENTS

LIST OF TABLES .....	viii
LIST OF FIGURES .....	ix
CHAPTER ONE.....	1
INTRODUCTION.....	1
CHAPTER TWO.....	3
ASSESSING VALIDITY OF FARMER RESPONSES TO ARMYWORM INFESTATION IN EJURA, GHANA: A STATISTICAL AND REMOTE SENSING APPROACH .....	3
Abstract .....	3
2.1. Introduction .....	4
2.2. Data and methods .....	7
2.2.1. Study Area .....	7
2.2.2. Armyworm infestation conceptual model .....	8
2.2.3. Farm Surveys .....	10
2.2.4. DEM .....	11
2.2.5. Enhanced vegetation index .....	11
2.2.6. Statistical Analysis .....	12
2.3. Results .....	12
2.3.1. Proportion of variance and loadings .....	12
2.3.2. Assessing the data structure via biplots .....	13
2.3.3. Statistical model .....	14
2.4. Discussion .....	14
2.5. Conclusions .....	16
CHAPTER 3 .....	19
COMPARISON OF ENHANCED VEGETATION INDEXES FROM LANDSAT 8 AND PARROT SEQUOIA MULTISPECTRAL CAMERA.....	19
Abstract .....	19
3.1 Introduction .....	20
3.2. Methods .....	22
3.2.1. Study Area .....	23
3.2.2. Image Preprocessing and EVI Calculation .....	23
3.2.3. Resampling and Alignment.....	24
3.2.4. Comparison and Modeling.....	24
3.3. Results .....	25
3.4. Discussion.....	30

3.4. Conclusion .....	30
CHAPTER 4 .....	32
CONCLUSIONS .....	32
REFERENCES .....	35

## LIST OF TABLES

Table 2.1: Regional statistics of African Armyworm Infestation .....	4
Table 2.2: Data sets used .....	9
Table 2.3: Statistical results from PCA on independent variables .....	13
Table 2.4: Loading for PC1, PC2 and PC3 .....	13
Table 2.5: Summary table for logistic regression analysis .....	14
Table 3.1: Results from linear regression analysis .....	27
Table 3.2: Results from linear regression analysis on predicted EVI .....	28

## LIST OF FIGURES

Figure 2.1: Map of Ejura showing locations of surveyed farms (upper right insert: Map of Ghana).....	9
Figure 2.2: Conceptual model of Armyworm infestation on maize and remote sensing .....	10
Figure 2.3: Model builder for clipping and extracting EVI mean and standard deviation for each farm.....	11
Figure 2.4: Biplots for PC2 versus PC1 and PC3 versus PC2.....	14
Figure 3.1: Map of Ejura showing location of the study area (upper right insert: Map of Ghana) .....	23
Figure 3.2: Flow diagram of methods used .....	25
Figure 3.3: EVI maps and histogram for Landsat 8 and Parrot Sequoia: (a) Landsat 8 EVI map (b) Parrot Sequoia EVI2 map (c) Landsat 8 EVI histogram (d) Parrot Sequoia EVI2 histogram .....	26
Figure 3.4: Map and histogram of EVI-EVI2 residuals respectively .....	27
Figure 3.5: Scatterplot of EVI and EVI2 as well plot of residuals versus fitted values .....	28
Figure 3.6: Predicted EVI map, observed EVI (first row from left to right respectively), difference between observed EVI and predicted EVI maps and histogram .....	29
Figure 3.7: correlation for observed and predicted EVI values.....	29

## **CHAPTER ONE**

### **INTRODUCTION**

African armyworms (*Spodoptera exempta*), although believed to have originated in North America, are most associated as a major crop pest in the continent of Africa, which recorded its first African armyworm infestation in the 1940s (Rose *et al.*, 1987). In recent years the country of Ghana has been heavily impacted by outbreaks of these crop pests. In 2017 Ghana lost a total of 18,000 hectares of cropland to the African armyworm menace (Ghanaweb, 2017). Given such high levels of infestation which threaten food security not only within Ghana but across the globe, several intervention mechanisms have been developed, proposed and implemented by researchers such as Brown (2015) and Faithpraise *et al.* (2015). Field surveys and remotely sensed data have been paramount to the success of these intervention mechanisms. While field surveys have been used to populate databases that have variables such as yield, levels of infestation, years of infestation, farm size, pest management practices to mention but a few, the utility of remote sensing has been explored via computation of vegetation indices. The normalized differential vegetation Index (NDVI) stands out in this regard. Several researchers have used NDVI to measure vegetation loss due to crop pest and subsequently related their findings to a loss in crop yield (Wilson and Gatehouse, 1992; Acharya and Thapa, 2015).

Although the application of field surveys and remote sensing to detection and monitoring of crop pests is important, uncertainties and inaccuracies within the data sources need to be addressed if accurate and insightful conclusions are to be achieved. Uncertainties and inaccuracies in remotely sensed data may be as a result of cloud cover, gaps in the temporal resolution of images, and variation in image spatial resolution (Zhu and Woodcock, 2012). While the first problem is an ongoing challenge for the satellite remote sensing community, problems from the other two can be mitigated by a combination of different sources of remotely

sensed data (UAVs, WorldView-2, Sentinel, Landsat, etc.). Field surveys are also subject to inaccuracies and uncertainties due to the structure of the questionnaire as well as responses obtained from respondents (Tessier, 2012).

The goal of this study is to validate the relationship between information obtained from farmers on the subject of African armyworm infestation via remote sensing and statistical techniques. Chapter 2 of this thesis discusses a research project to assess the relationship between farmers' responses to African armyworm infestation in Ejura, Ghana and vegetation metrics from satellite remote sensing. A total of 67 farm sites were sampled for inclusion in a logistic regression analysis. These farms were partitioned into 51 training sites and 18 testing sites. Since the goal in this chapter was to ascertain if remotely sensed data are good predictor variables for armyworm infestation, only slope and Landsat 8 EVI values constituted predictor variables while farmers' responses to the presence or absence of armyworm infestation (presence=1, absence=0) served as the dependent variable.

The goal of Chapter 3 was to provide a solution to the issue of cloud cover in satellite-based remote sensing. A linear regression model was developed using Landsat 8 and resampled Parrot Sequoia EVI2 and was subsequently tested on a section of the study area (about 17 acres). A relatively novel approach was developed to rescale EVI2 from Parrot Sequoia to EVI from Landsat 8. Achieving this was based on understanding how the pixel values in the Landsat 8 image were obtained. This approach, therefore, facilitated the comparison of these two indices even though the spatial resolutions were so different. Comparing EVI and EVI2 in this study context serves as another novel attribute of this research

## CHAPTER TWO

### ASSESSING VALIDITY OF FARMER RESPONSES TO ARMYWORM INFESTATION IN EJURA, GHANA: A STATISTICAL AND REMOTE SENSING APPROACH

#### **Abstract**

Since the 1960s, Sub-Saharan Africa has experienced an influx of African armyworm infestation, including the country of Ghana. Three political regions in Ghana have experienced the highest crop losses: Brong Ahafo (Eastern), Volta and Northern. While regional agricultural loss assessments are available through field surveys, these surveys are subject to considerable uncertainty in regards to the spatial extent and timing of infestation due to the lack of robust applications of geospatial and statistical methodologies. This research therefore uses a combination of remote sensing and statistical techniques to assess the uncertainty in factors involved in African armyworm infestation on maize and their extent in Ejura, Ghana. Specifically, this research uses regression analysis to validate survey responses about armyworm infestation reported by farmers in Ejura for the farming season of 2017. To achieve this, principal components derived from mean Enhanced Vegetation Index (EVI) obtained from the Landsat 8 level 2 product for the months of April, May and July as well as mean slope of the study area were regressed against presence or absence of armyworm infestation. Although this model did not incorporate other significant parameters such as the entire maize phenological cycle (from April to September), fertilizer usage, or soil type an armyworm infestation prediction model was developed with a 61 percent prediction accuracy for a validation dataset. This work therefore shows that making decisions in relation to African armyworm infestation from only remotely sensed information or field surveys could lead to biased interpretation.

## 2.1. Introduction

Food security is a complex topic which involves demand factors such as population growth, urban migration, and change in diet, and also supply factors, including number and size of farms, total arable land extent, agricultural technology, impact of climate variability and change, and other effects on yield. To help tackle this issue, there has been tireless efforts across the world to ensure warning systems are in place to help grow, process and store food, while other factors such as climate change, land use land cover change and pest control continue to pose problems. Crop pests in particular are very important to understand because of their potential to devastate crops especially in parts of the world that depend on these crops for their food source (SC and Echezona, 2012; Bebber *et al.*, 2014).

One pest that has gained notoriety in food security over the past decades is the African Armyworm (*Spodoptera exempta*). The African Armyworm has impacted food security in African and more specifically Ghana in recent years (Rose *et al.*, 1997; Sibanda, 2004). A report by Nboyine *et al.*, (2017) showed that over 4,900 hectares of cropland in Ghana were devastated by African Armyworm in 2016, and approximately \$164,000,000 of crop yield losses were recorded in 2017 as reported in Table 2.1.

**Table 2.1: Regional statistics of African Armyworm Infestation**

<b>Region</b>	<b>Infestation Extent (hectares)</b>
Brong Ahafo	14,201
Eastern	1,583
Ashanti	365
Central	1,349
Greater	117
Northern	354
Upper West	6
Volta	227
Western	15
<b>Total</b>	<b>18,217</b>

Source:(Ghanaweb, 2017)

The life cycle of the Africa armyworm revolves around four phases: egg, larvae and pupating, adult moth stages. The larvae stage, which spans between 14-22 days after the eggs of a moth are hatched, represents a voracious period of the organism's life cycle ( Johnson, 1987; Idrissa *et al.*, 2017). According to Barlow and Kuhar, (2009), Barlow & Kuhar, (2009) and Capinera, (2017), maize leaves are among the favored foliage consumed by African Armyworms, thus affecting the phenology of the maize and resulting in the maize plant's inability to carry out photosynthesis.

The magnitude and extent of pest damage on crop yield has motivated a range of research on monitoring and modeling the effect of crop pests via remotely sensed data. However, while remotely sensed information has been applied over the years to investigate the spatial distribution of a variety of crop pests (e.g., Yang *et al.*, 2009; Prabhakar *et al.*, 2013; Lausch *et al.*, 2013; Asiedu *et al.*, 2017), investigations of African armyworm infestation within sub-Saharan Africa are uncommon. A review of existing literature shows that while works such as Riley, (1989) and (Pisani *et al.*, 2000) presented a conceptual frame work that could address the issue of African armyworm infestation through remote sensing, only Adama and Mochiah, (2017) applied these frameworks in Western Africa.

At fine spatial scales, an object oriented approach was used by Alvarez-Taboada, *et al.*, (2017) to identify and quantify the habitat and distribution of invasive plant species. Classification of crop cover produced from Unmanned Aerial Vehicle (UAV), or drone was compared with classifications from images obtained via orbital platform (WorldView-2: WV2) data sets. The results from WV2 classifications showed accuracies above 95% while UAV images produced classification above 75%. At broader spatial scales, Adama and Mochiah, (2017) used normalized Vegetation Index (NDVI) from MODIS, rainfall data and temperature data to assess the relationship between outbreaks of the African armyworm and climatic factors in the forest transition zone of Ghana. Their research revealed that NDVI values were low

during times when African armyworm infestation occurred in the study area amidst favorable weather conditions.

Although studies have been conducted to justify significant drops in vegetation greenness while controlling for precipitation and temperature, no research has investigated armyworm infestation in relation to enhanced vegetation index (EVI). In theory, EVI could be more suitable than NDVI for studies of African armyworm infestation on maize (Huete *et al.*, 2002): while NDVI estimates leaf area index in canopies without compensating for effects of soil background, EVI estimates leaf area index by differentiating soil background from vegetation in low ground cover areas. EVI therefore should estimate spectral values that truly reflect the vegetation cover without the influence of soil spectral values. EVI can be calculated for pixels in multiband imagery with the following equation:

$$EVI = G \frac{(NIR - Red)}{NIR + (C1 * Red - C2 * Blue) + L} \quad (1)$$

Where  $L$  is a soil adjustment factor and  $C1$  and  $C2$  are coefficients used to correct aerosol scattering in the red band by the use of the blue band. The Blue, Red, and NIR represent reflectance at the blue (0.45-0.52 $\mu$ m), red (0.6-0.7 $\mu$ m), and near-infrared (NIR) wavelengths (0.7-1.1 $\mu$ m), respectively. In general,  $G=2.5$ ,  $C1=6.0$ ,  $C2=7.5$ , and  $L=1$  (Matsushita *et al.*, 2007).

Although very insightful findings about crop pests can be obtained from remotely sensed data, making inferences from remote sensing data without some form of ground truth can be misleading (Bobbe *et al.*, 2001; Miyazaki *et al.*, 2011). One way of providing reference data for remotely sensed data analysis is with field surveys, and this approach has been explored in several studies ( e.g., Abteu *et al.*, 2016; Osgood *et al.*, 2018; Caiserman *et al.*, 2019). However, surveys are also subject to errors. Vidich and Bensman (1954) grouped

sources of errors from the respondent into 4 broad categories: 1) purposeful intent, which refers to the respondent's intent to give better impression of a situation via slanted information; 2) temporary role of respondent, which occurs when the respondent gives answers with the intention of helping the researcher to solve a specific problem; 3) psychology of respondent, which refers to situations where the respondent is subject to failure of and selectivity of memory recall; and 4) involuntary error, which addresses situations where the respondent is unable to give accurate answers due to constraint or blockages resulting from the structure of the interview. This study appears to be the first to attempt to validate farm interview responses with remotely sensed data applied to African armyworm infestation.

This research therefore seeks to use a combination of remote sensing and statistical techniques to unravel the uncertainty in questionnaire response about African armyworm infestation in maize in Ejura, Ghana. Specifically, this research uses a two-step statistical approach to validate farmers' responses to a question relating to armyworm infestation. In the first step, collinearity between five variables (maize yield in 2017, slope, EVI for April, May and July 2017) for 69 farms is reduced through Principal Component Analysis (PCA). The second step employs logistic regression analysis to develop a model that uses farmers' responses to a question regarding presence/absence of infestation for 2017 as a dependent variable and an informative subset of principal components from step one.

## **2.2. Data and methods**

### **2.2.1. Study Area**

The study area is in the district of Ejura-Sekyedumase, located in the northern part of the Ashanti Region of Ghana and situated within longitudes 1°5' W and 1°39' W and latitudes 7°9' N and 7°36' N (Figure 2.1). The total population of the district is approximately 85,000 people, a majority of whom are less than 15 years of age. The work force (ages 20-64)

comprises 43.2% of the population. Ejura-Sekyedumase has an average annual temperature range between 26.4 and 27.5°C while its average annual rainfall is between 1,200 mm – 1,500 mm. The chief rainy season occurs between April and November. However, the drier dusty wind, which results from northeast trade winds, occurs during the dry season (December to March). As an area located in the transition zone, the main vegetation cover is comprised of both grassland and woodland with broadleaf trees (Morton, 2013). The principal economic activity of the study area is agriculture, including crop farming, poultry keeping, and cash tree plantations such as teak trees. Beans, maize and rice are planted in crop rotation fashion to help retain nitrogen in the soil. The main crops are plantain, maize, yam, rice, beans, cassava, groundnuts and watermelon, with maize and watermelon constituting dominant commercial crops (Asiedu *et al.*, 2017).

### **2.2.2. Armyworm infestation conceptual model**

The mechanism behind the armyworm infestation within the study area is summarized by the model in figure 2.2. The process commences with the cultivation of maize by farmers. Once the maize develops foliage, it becomes a potential food source for the African armyworm (Holt, 2004). However, wind speed and temperature need to be suitable to enable the armyworms to be transported via wind from a location of origin to a maize farm of interest (Wilson and Gatehouse, 1992). The time lapse between the sowing, growing and harvest of the maize on the farm is pivotal in this research.

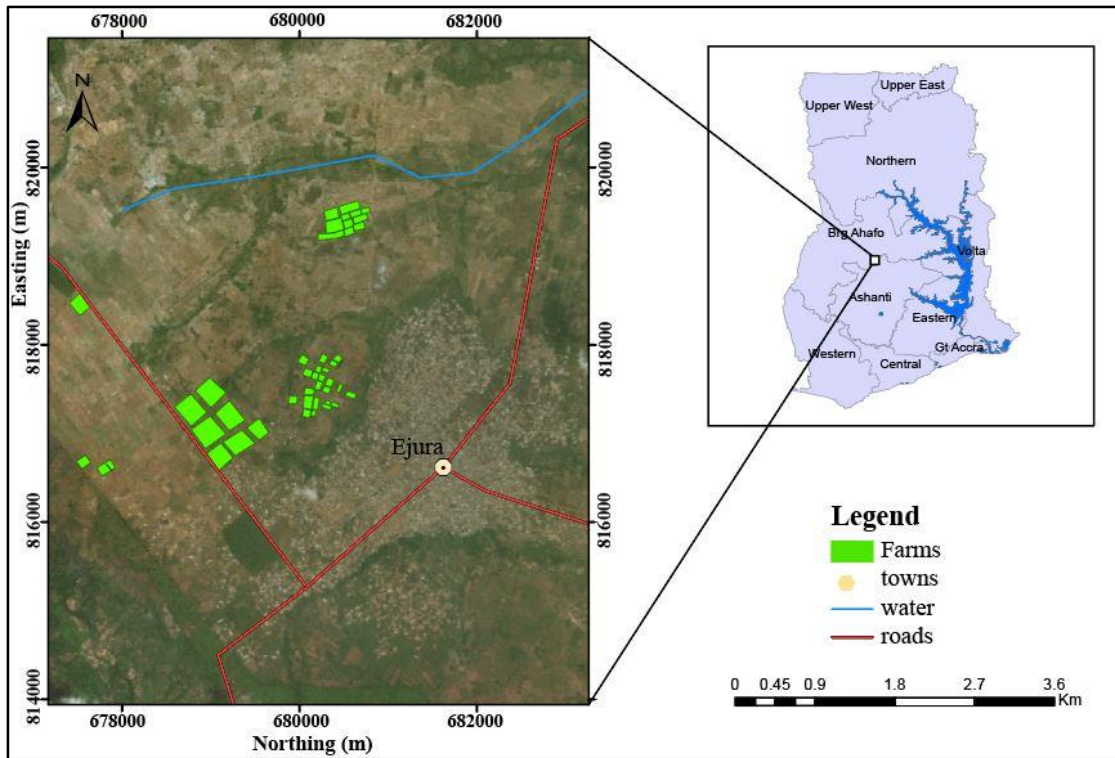


**Figure 2.1:** Map of Ejura showing locations of surveyed farms (upper right insert: Map of Ghana)

With the advent of satellite images and pre-processed vegetation index products such as MODIS, the various stages of the maize phenology can be extracted from reflectances received and reflected by the maize crop (Justice *et al.*, 2007; Griffiths *et al.*, 2019). Figure 2.2 proposes that remote sensing is able to capture both the maize planting and growing cycles as well as signals for the infestation of African armyworms, thus making remote sensing a reliable source of information. Against this background, the various sources of data for summarized in table 2.2 were used for this work.

**Table 2.2:** Data sets used

Data	Scale	Source
EVI	30 m	USGS Landsat 8 OLI/TIRS C1 Level-2
DEM	30 m	USGS
Farm demographics	N/A	Farm survey during summer April-July 2018

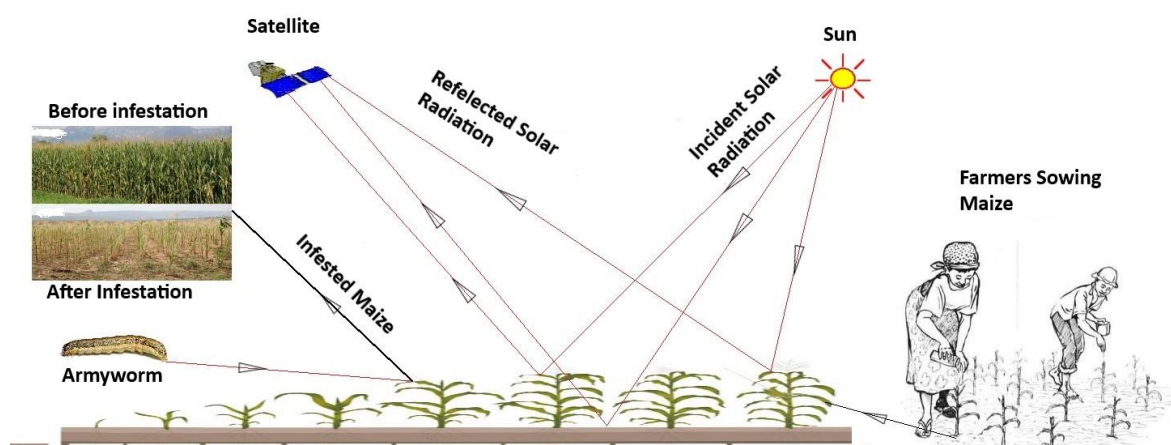


**Figure 2.2:** Conceptual model of Armyworm infestation on maize and remote sensing

### 2.2.3. Farm Surveys

IRB certification (ID: STUDY00000653) was obtained from Michigan State University to interview a random sample of 75 farmers from the Ejura farming community between the months of May and July 2018 with a team of four field technicians with me as the team leader. To ensure the homogeneity among data collected by field technicians, I organized a training session to educate them on how to effectively and efficiently ask questions and write down responses with minimal ambiguity. This I achieved by allowing the field technicians to mock the interviews with some farmers in my presence and subsequently correcting them on areas where I could sense ambiguity in how the questions were asked and responses documented. Information pertaining to farm size (in acres), age of farmer, crops planted, maize yield and level of armyworm infestation during the 2017 farming period were obtained from field surveys. Out of 75 farms, six had to be eliminated from further analysis because they were periodically situated in densely clouded areas on available imagery for the study. It is also important to state that variables such as precipitation, temperature, infestation from other crop pests and weed management practices which could have improved the results of this study were not included in the field interviews. (For meteorological variables this omission was due to their lack of variation over the small (~20 km<sup>2</sup>).

#### 2.2.4. DEM

A digital elevation model (DEM) for Ejura was obtained from an ASTER Global DEM file hosted on the USGS website (EarthExplorer). ArcMap was used to clip out slope and elevation values for each farm. Since the ultimate goal was to extract summary statistics such as mean and standard deviation for elevation and slope, raster summaries of these values for each farm were calculated.

#### 2.2.5. Enhanced vegetation index

While substantial efforts were made to obtain satellite imagery that represented the whole maize phenological cycle, only pre-processed EVI products for the months of April, May, and July (during 2017) from the United State Geological Survey (USGS) website were cloud-free enough for inclusion in this work. This dataset was also used because all necessary corrections required to make quantitative and qualitative inference had already been carried out. After standardizing the EVI values by multiplying each raster by 0.0001, mean of EVI for each farm was obtained after farm polygons were used to clip out the farm areas. Given the large number of farms (69) that needed to be clipped for a total of 9 EVI raster maps, a model was developed in ArcMap Model Builder to help automate the process (Figure 2.3).

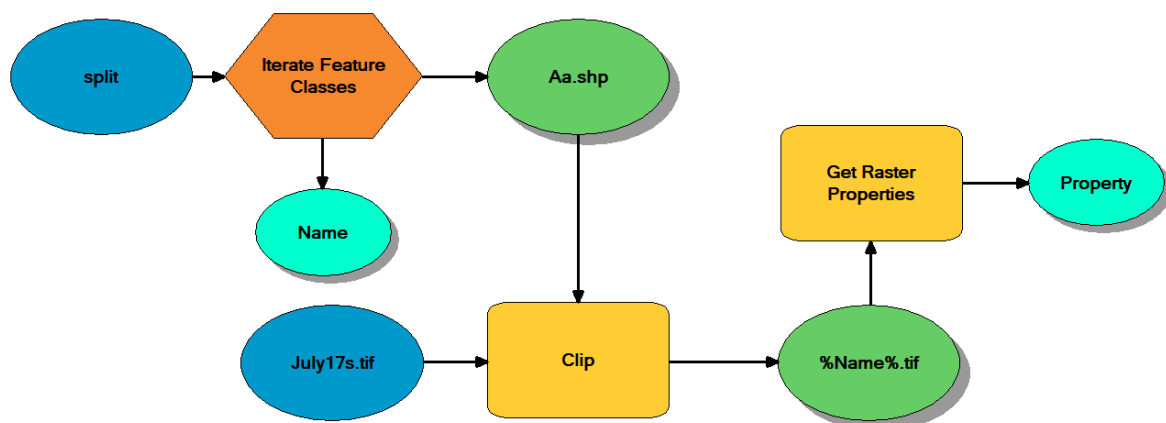


**Figure 2.3:** Model for clipping and extracting EVI mean and standard deviation for each farm

### **2.2.6. Statistical Analysis**

Reduction in multi-collinearity among the seven independent variables (mean EVI for April, May, and July, difference between May and April, difference between July and May, difference between July and April and mean slope) was achieved through principal components analysis (PCA). To ensure that the independent variables met the requirements for PCA, the variables were first standardized to ensure equal distribution of variance. Three principal components were selected based on their cumulative proportion of variance. These components were PC1, PC2 and PC3. 51 training and 18 testing sites were randomly selected for further analysis. Next, a logistic regression analysis was conducted on the training samples. Farmers' responses to the presence or absence of armyworm infestation served as the dependent variable and regressed against the three selected principal components. A model was developed from the training data set used to predict the testing data sets. To achieve a high success rate for the developed model, Receiver Operating Characteristic (ROC) graphs were used to obtain a suitable threshold of 0.81 and fed into the predicting model. ROC graphs were used because the ability of a model to be unbiased or biased towards a specific prediction can be readily obtained.

## **2.3. Results**

### **2.3.1. Proportion of variance and loadings**

Cumulative proportion of variance resulting from the PCA revealed that PC1, PC2 and PC3 explained the majority of the variance in the independent variables, as shown in Table 2.3: these were chosen for subsequent analysis. Loadings of the first three principal components are shown in Table 2.4. Mean EVI for July, difference between July and May as well as that between July and April were positively correlated with PC1, while mean EVI values for May were negatively correlated. In contrast, PC2 was positively correlated with mean EVI in May

and negatively correlated with mean slope and with difference in mean EVI between May and April. Mean slope was the only variable that displayed a negative correlation with PC3.

**Table 2.3:** Statistical results from PCA on independent variables

	PC1	PC2	PC3	PC4	PC5	PC6	PC7
Standard Deviation	1.9357	1.3142	0.8834	0.8636	5.48e-16	3.6e-16	1.60e-16
Proportion of Variance	0.5353	0.2467	0.1115	0.1065	0.0000	0.0000	0.0000
Cumulative Proportion	<b>0.5353</b>	<b>0.7820</b>	<b>0.8935</b>	1.0000	1.0000	1.0000	1.0000

**Table 2.4:** Loading for PC1, PC2 and PC3

Variables	PC1	PC2	PC3
April EVI	0.0717	<b>0.6459</b>	-0.1266
May EVI	<b>-0.4258</b>	-0.0636	0.2923
July EVI	<b>0.4640</b>	-0.1044	0.2628
May-April EVI	-0.3968	<b>-0.4274</b>	0.3173
July-May EVI	<b>0.5152</b>	-0.0438	0.0502
July-April EVI	<b>0.4182</b>	-0.3847	0.3103
Slope	0.0229	<b>-0.4851</b>	<b>-0.7937</b>

### 2.3.2. Assessing the data structure via biplots

Figure 2.4 gives a visual representation of the data structure as explained for PC1, PC2 and PC3. Both plots show that an multicollinearity between the original variables has been removed in the principal components. The plots also support the description of the loadings discussed in section 2.3.1.

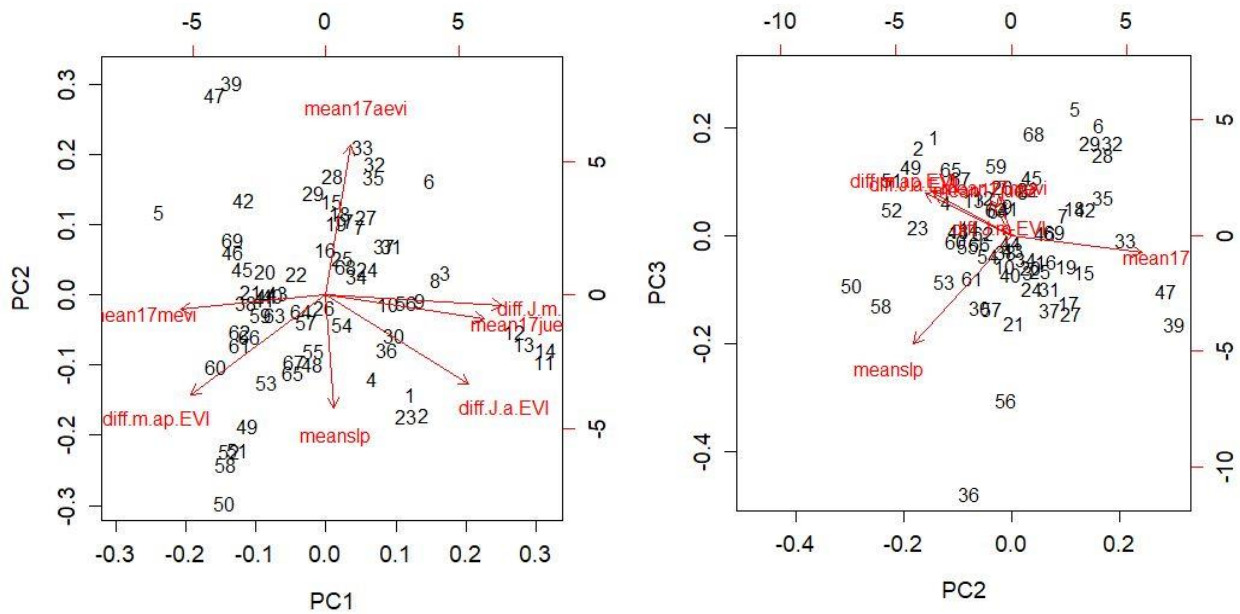


**Figure 2.4:** Biplots for PC2 versus PC1 and PC3 versus PC2

### 2.3.3. Statistical model

Equation 1 represents the model that was used to produce the results displayed in Table 2.5. Standard errors for each coefficient were large and the large p-values indicated that there was no correlation between the dependent variables and independent variables.

$$\text{Infestation} = 0.08\text{PC1} - 0.12\text{PC2} - 0.36\text{PC3} + 1.61 \quad (1)$$

**Table 2.5:** Summary table for logistic regression analysis

Variables	Coefficients	Estimate Std. Error	z value	Pr(> z )
PC1	0.07908	0.20139	0.393	0.695
PC2	-0.10219	0.28758	-0.355	0.722
PC3	-0.35946	0.46787	-0.768	0.442

## 2.4. Discussion

Validation of field surveys in relation to agriculture practices has been explored in several research works and yielded very informative results (Nespeca *et al.*, 1997; Midega *et*

*al.*, 2012; Abteu *et al.*, 2016). Similarly, crop pest distribution has been characterized with remotely sensed data in research activities such as Eklundh *et al.*, (2009) and Rai and Ingle, (2012). In this work I developed a prediction model for Armyworm infestation within the northern part of Ejura, Ghana using a combination of methods. I achieved this by regressing farmers' response to the presence or absence of African armyworm infestation with three principally reduced independent variables.

Visual inspection of loadings for the principal components revealed that PC1 had a positive correlation with EVI values for difference between July and April as well as July and May. While similar observation can be made for EVI for July, EVI value for May appeared to be negatively correlated with PC1. This pattern was interpreted as PC1 measuring not only monthly variations in vegetation greenness but early changes in vegetation change. PC2 had high positive correlation with April but registered negative correlation with slope and difference in EVI for May and April (-0.4851 and -0.6459 respectively). PC2 therefore captured earlier maize phenology strongly suggesting that it is a good predictor of how terrain affects reflectance from vegetation (bidirectional reflectance distribution function, or BRDF). A high negative correlation with slope was observed for component 3 (-0.7937) and this was associated with either a sharp decrease or increase in slope within the farms.

P-values from the logistic regression analysis for PC1, PC2 and PC3 (0.695, 0.722 and 0.442 respectively) showed that the betas were not significantly different from zero, indicating no linear relationship with the dependent variable. Despite the absence of correlation between the dependent variable and independent variables, the prediction phase of the analysis was carried out on the validation dataset. At this stage I would like to suggest possible reasons for the lack of correlation between the dependent and independent variables. One possibility is that, there were inaccurate responses from farmers during the surveys. This could be as a result of farmers being biased toward responding 'yes' to presence of infestation in anticipation for

some form of reimbursement from the government. If this is the case, then the research hypothesis that EVI values reflect the degree of armyworm infestation is incorrect. A second possibility is that the absence of EVI values for the whole maize seasonal cycle could be a contributory factor. In this case obtaining EVI values for each of the two 16-days composite (Landsat 8) in a month would be a more accurate representation of the phenology of maize in the study area. In addition, using EVI values from sensors such as Sentinel (10 and 20 m spatial resolution and temporal resolution of 5 days), WorldView-2 (0.46 m spatial resolution), or UAVs (varying but very high spatial resolution), might be capable of capturing changes in vegetation more accurately. The reader is however cautioned against the perilous effect of cloud cover in remotely sensed images which was inevitable in our case. Cloud cover issues proved challenging in this work due to the following reasons: 1) cloud cover was a challenge for observation interval in many places; 2) the study site selected for this work is tropical, and subject to dense cloud cover during the growing season; 3) this project required extensive assessment of the Landsat archives to find scenes cloud-free enough to work. The reader is however encouraged to employ the methodology exhibited in this work to validate and selected parameters for African armyworm prediction and modeling activities.

## **2.5. Conclusions**

This research has brought to bear the potential and limitations of validating field surveys in relation to African armyworm via remotely sensed data and statistical analysis. Most importantly the findings indicate that assuming vegetation change measured from satellite sensors directly translates to pest infestation is not always the case. This is evident in the insignificant p-values that were observed from the logistic regression analysis. However, this research work is also the first to address the issue of African armyworm infestation while validating the sources of data sets through statistical methods and also using EVI instead of NDVI. Admittedly, the model explored in this work did not perform well; nevertheless, the

reader's attention is brought to the techniques and methodology employed in arriving at the goal of this research. Several factors could have affected the outcome of this study and I would like to address some of these factors. Primarily, not being able to obtain EVI values that would represent the entire phenology of maize (April-September) within the study area affected the results of this work. While the phenology of maize in Ejura spans over 7 months, only three of these months (April, May and June) were used in this study. Shadow as a result of cloud cover in the satellite imagery could also impacted the results. Even though conscious effort was made to eliminate cloud cover-prone farms from the initial dataset, effects of shadow resulting from clouds was not addressed in this work. It is therefore possible that some of the EVI values observed were affected by shadows from cloud cover. Other weather conditions such as drought cloud also be driving the changes in EVI values that were observed. Since this factor was not controlled for by incorporating climatic data such as precipitation and temperature, changes in EVI can not necessarily be assigned to armyworm infestation. The last factor that could have impacted the results reported in chapter two is difference in farm management practices. A typical example in this sense would be weeding. Weeds have the potential to contribute to the total biomass of vegetation observed for a specific field and EVI for that matter. The possibility of the farmers interviewed for this work practicing different weed control practices cannot be overruled and therefore have a potential effect on the findings from this study.

Researchers are therefore advised to tread cautiously when making inferences from only field surveys or remotely sensed information in relation to crop pests, especially concerning African armyworm infestation on maize. Future work is encouraged in this field with similar techniques described in this work but with other variables such as precipitation, temperature and wind speed which are all factors affecting the activities of African armyworm. Increasing the sample size of the study area with similar methodology is also encouraged, given

that this might give the research a better confidence interval for the true representation of the total population.

## CHAPTER 3

### COMPARISON OF ENHANCED VEGETATION INDEXES FROM LANDSAT 8 AND PARROT SEQUOIA MULTISPECTRAL CAMERA

#### Abstract

The presence of earth orbiting satellites such as Landsat and MODIS that constantly produce remotely sensed imagery may complement the increasing application of imagery from unmanned aerial vehicles (UAVs) in precision agriculture. A vital question is whether information obtained from satellite imagery can be compared with similar data obtained from UAVs given fundamental differences between these sensors. This study compares Enhanced Vegetation Index (EVI) obtained from the Landsat 8 level 2 product with EVI2 calculated from a Parrot Sequoia multispectral camera deployed on a DJI Phantom 4 pro drone. The aim of this approach is to validate the robustness of the EVI2 equation for low altitude sensors such as multispectral cameras deployed on UAVs. The study site is Ejura, a predominantly maize farming community situated in the Ashanti region of Ghana, during the month of July, 2018. Findings from this research showed that there was a positive correlation between EVI and EVI2 (with an adjusted R-squared of 0.59). Residuals from the difference between EVI and EVI2 followed a bell-shaped distribution with the following observed geographic patterns: (1) higher residuals distributed around the edges and south-western section of the study area; (2) lower residuals situated predominantly in the central section of the study area. The validation stage of the model that was developed indicated that the model could predict EVI for Landsat 8 (from Parrot Sequoia EVI2) with about 61% accuracy. A map of the residuals between observed EVI values from Landsat and predicted EVI values from the model depicted lower residuals in areas with homogeneous vegetation than in areas that had heterogeneous vegetation (especially areas with a mixture of dry and green maize foliage). This observed pattern was strong even given a small time lag between the date of drone image acquisition and Landsat 8 image acquisition.

### 3.1 Introduction

Applications of satellite-based remote sensing span many industries including mining, construction, and agriculture. Several research papers (Miller and Small 2003; Turner *et al.*, 2003; Melesse *et al.*, 2007; Rajitha *et al.*, 2007; Klemas 2013) have looked at the applications of satellite-based remote sensing in both the private and public sectors and made remarkable and insightful revelations. In fact, a visit to EarthExplorer which is hosted on the United State Geological Survey (USGS) website reveals a conscious effort to make remotely sensed data from satellite imagery readily accessible to both the private and public sector. With the aid of a friendly user interface, visitors to the EarthExplorer home page can access and download a myriad of post- and pre-processed data that characterize terrain, climate, land use and land cover, and raw satellite imagery for the whole globe. Similarly, the Moderate Resolution Imaging Spectroradiometer (MODIS) project has a website that allows customization of satellite imagery, for rapid download. Although these approaches adopted by traditional satellite data hosting websites such as MODIS and USGS continues to be actively patronized (Wulder *et al.*, 2012), acquiring remote sensing data from UAVs is gaining currency in the twenty-first century (Hackney and Clayton, 2015).

Proponents of the application of UAVs in remote sensing argue that they offer high resolution, high quality information that can be acquired at any given time without cloud cover issues. These characteristics make UAV-based imagery a competitor to satellite dependent remote sensing (Xiang and Tian 2011; Torres-Sánchez *et al.*, 2014; Stöcker *et al.*, 2017). Also the availability of desktop UAV data processing software such as PIX4D, Global Mapper, DroneDeploy and Agisoft makes processing of UAV imagery a less laborious process. Currently a substantial number of low budget UAVs on the market do not come with built-in multispectral cameras. This is unfortunate, since multispectral image data have many applications in precision agriculture and land use land cover change analysis (Torresan *et al.*,

2017; Fernández-Guisuraga *et al.*, 2018). Third party companies such as Parrot and MicaSense produce multispectral cameras that fall within the budget range of customers who cannot afford more expensive multispectral cameras, which may cost as much as \$60,000. This symbiotic relationship between UAV manufacturing companies and multispectral sensor production firms has revolutionized the application of UAVs in precision agriculture (Lelong *et al.*, 2008; Garcia-ruiz *et al.*, 2013; Honkavaara *et al.*, 2013; Candiago *et al.*, 2015; Roosjen *et al.*, 2018; Mogili and Deepak 2018).

Ahmed *et al.*, (2017), in research that deployed a Parrot Sequoia multispectral camera on a UAV, classified land cover in Peterborough, Ontario into five land use land cover classes (forest, shrub, herbaceous, bare soil, and built-up); an overall classification accuracy of 95% was reported. Tang (2015) proposed the term ‘drone remote sensing’ to refer to the increasing application of drones for remote sensing. Their paper discussed the applications of drone imagery in forest canopy gap surveys, forest canopy height measurements, and tracking of forest wildfires. In a study of vegetation indices for two Italian vineyards, Matese *et al.* (2015) compared normalized differential vegetation index (NDVI) obtained from satellite imagery, drone deployed multispectral imagery and aircraft imagery. Findings from their work showed that NDVI from the three methods were comparable in homogenous vineyard sections but substantially different for heterogeneous sections of the vineyard. Several other papers (e.g., Baluja *et al.*, 2012; Das *et al.*, 2015; Kalisperakis *et al.*, 2015; Duan *et al.*, 2017) exemplify how NDVI has been derived and used from multispectral cameras deployed on UAVs.

Despite the simplicity of NDVI, which is calculated as the ratio of difference between the near infrared and the red band to the sum of the near infrared and red bands, and its extensive use (Matsushita *et al.*, 2007) it does have weaknesses. These weaknesses result from environmental effects such as soil background and atmospheric condition (i.e., the presence of aerosols). These drawbacks to NDVI led to the creation of the EVI algorithm (Xiao *et al.*, 2003;

Montandon and Small, 2008). EVI corrects for soil background and atmospheric effects, making it a good choice for measuring vegetation biomass across the globe (Rocha and Shaver, 2009). However, while research exists in support of EVI computations from satellite imagery (Zhu *et al.*, 2014; Peng *et al.*, 2017 ;Testa *et al.*, 2018), very little research has explored computation of EVI from multispectral sensor deployed on UAVs (Fang *et al.*, 2016). Given that applications of UAV deploying multispectral cameras for precision agriculture are increasing, it is in the interest of researchers and agricultural and remote sensing practitioners to explore the potential of the EVI2 equation proposed by Jiang *et al.*, (2008) for UAV deployed sensors.

This study compares two vegetation indices: EVI2 computed from a Parrot Sequoia multispectral sensor deployed on a DJI Phantom 4 pro drone, and EVI obtained from the Landsat 8 Level 2 preprocessed product. The comparison was achieved by developing a linear model that regressed EVI for Landsat 8 against EVI2 computed on resampled (30\*30m resolution) imagery from a Parrot Sequoia multispectral camera. The prediction phase of this research involved using the model developed to predict the spectral structure of a scene of the study area that was not included in the initial analysis. The study area is the agrarian community of Ejura, located in the Ashanti region of Ghana. It is worth mentioning that the main challenge of comparing information from the two sensors mentioned above is the difference in spatial resolution: Landsat 8 sensor has a spatial resolution of 30\*30 m while the Parrot Sequoia imagery flown in this study has a spatial resolution of 0.04\*0.04 m.

## **3.2. Methods**

### **3.2.1. Study Area**

The study region (see figure 3.1) is a predominantly agricultural area of about 123 (training site) and 17 (testing) acres located in the district of Ejura-Sekyedumase, in the

northern part of the Ashanti Region of Ghana. A bounding box with coordinates: 1°23' W, 7°23' N (upper left) and 1°22' W, 7°23'03'' N (lower right) describes the geographical location of the study area. The average annual temperature for the region ranges between 26.4 and 27.5 °C with an average annual rainfall between 1,200 mm – 1,500 mm. Maize, yam, rice, beans, cassava, groundnuts and watermelon are the main crops planted by farmers within the study area. However, maize and watermelon constitute the crops that are cultivated on a commercial basis (Asiedu *et al.*, 2017).

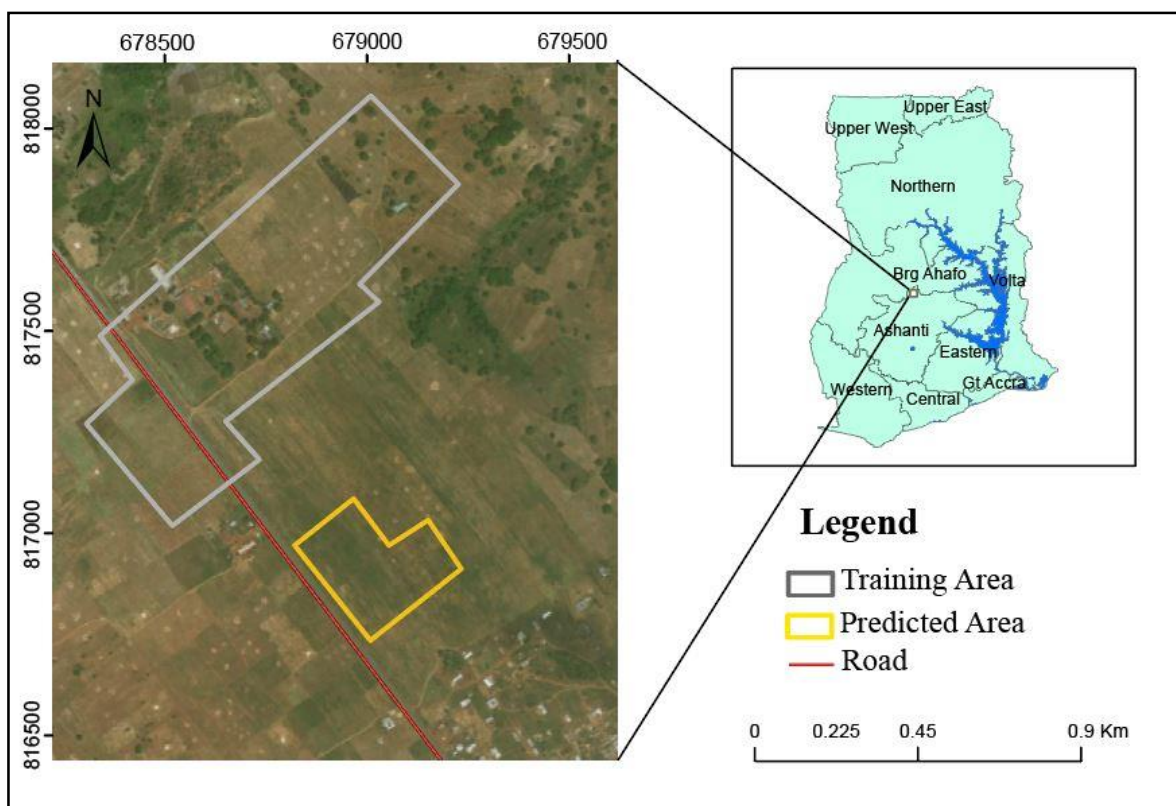


**Figure 3.1:** Map of Ejura showing location of the study area (upper right insert: Map of Ghana)

### 3.2.2. Image Preprocessing and EVI Calculation

Imagery obtained from Parrot Sequoia multispectral camera was processed in the Pix4D software environment. Multispectral image processing in Pix4D generally goes through three main processes (Initial process to develop cloud points, generation of digital surface modules and generation of orthophotos). The index calculator option was then selected, and a

customized EVI2 equation as proposed by Jiang et al. (2008) for the computation of EVI from a low altitude sensor was used to compute EVI for all images, as shown in Equation 3.1:

$$EVI2=2.5 \frac{(NIR-Red)}{NIR+(Red*2.4)+1} \quad (1)$$

Where NIR= Near Infrared band and Red=Red band from the multispectral camera.

### **3.2.3. Resampling and Alignment**

Since the pre-processed imagery obtained from USGS had EVI values at 30-meter resolution, all processed imagery from Pix4D mapper was resampled (nearest neighbor method) to 30 m resolution in ArcMap. Georeferencing was then carried out to ensure images from both sensors were aligned. To achieve this some landmarks were identified on images from both sensors and used as tie points with an overall accuracy of 0.18 m.

Next, the processed images from Parrot Sequoia sensor were used to clip the georeferenced Landsat 8 EVI imagery obtained from USGS. The clipping process was conducted with the “clip to extent” option selected in ArcMap. The final activity in ArcMap was to extract the EVI values from both Landsat georeferenced EVI imagery and resampled Sequoia EVI imagery. This was achieved by using the “convert from raster to point shapefile” tool.

### **3.2.4. Comparison and Modeling**

Finally, both EVI and EVI2 images were analyzed with the aid of the raster and statistical packages in R Studio (Hijmans, 2019; Team R, 2017). Maps and histograms for both EVI and EVI2 were developed for visualization. The next step was to develop a model for EVI prediction using EVI2 imagery. The model selected was an ordinary least squares regression model which was developed by regressing EVI2 against EVI. The model developed was then

used to predict the spectral structure of a Landsat 8 image of a section of the study area. The flowchart in figure 3.2 summarizes these processes

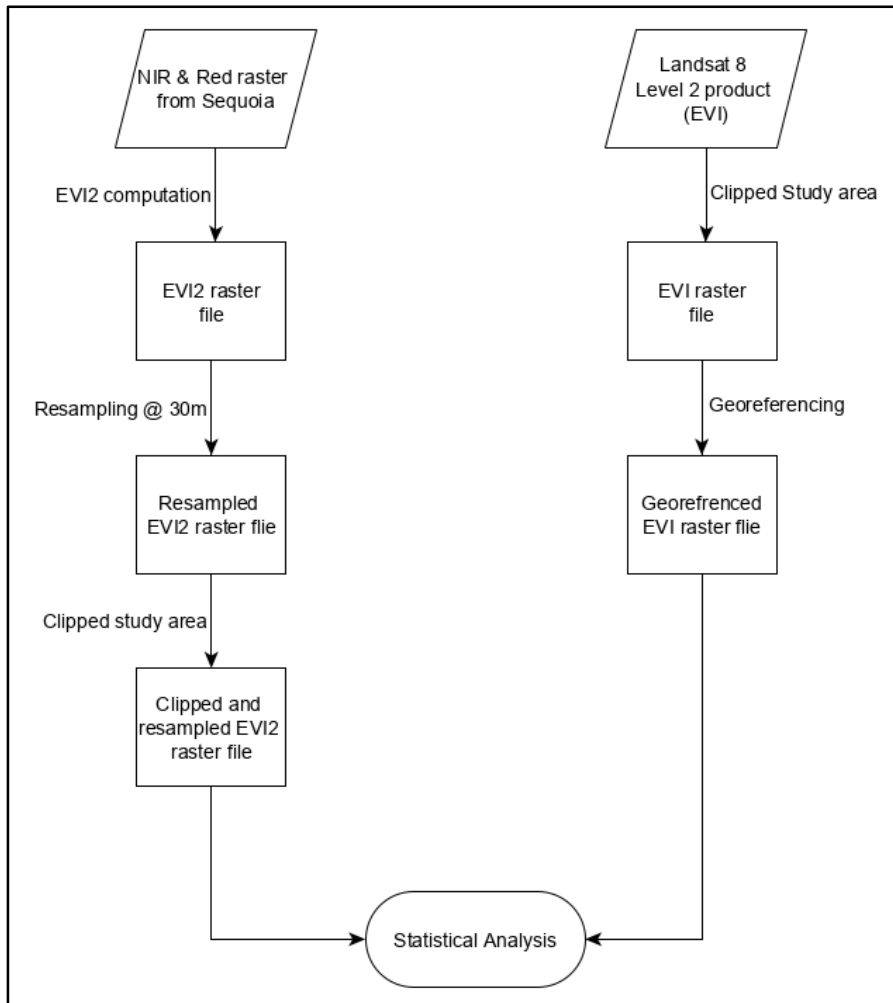


**Figure 3.2:** Flow diagram of methods used

### 3.3. Results

Plots for EVI and EVI2 maps showed that both maps were consistent in area with high plant biomass (south-western parts of the study area). In area with mixed maize phenology, the EVI2 map appeared to have high values as compared to the EVI map. Histograms for both sensors also showed a somewhat right-skewed distribution. Figure 3.3 shows maps and histograms for both sensors.

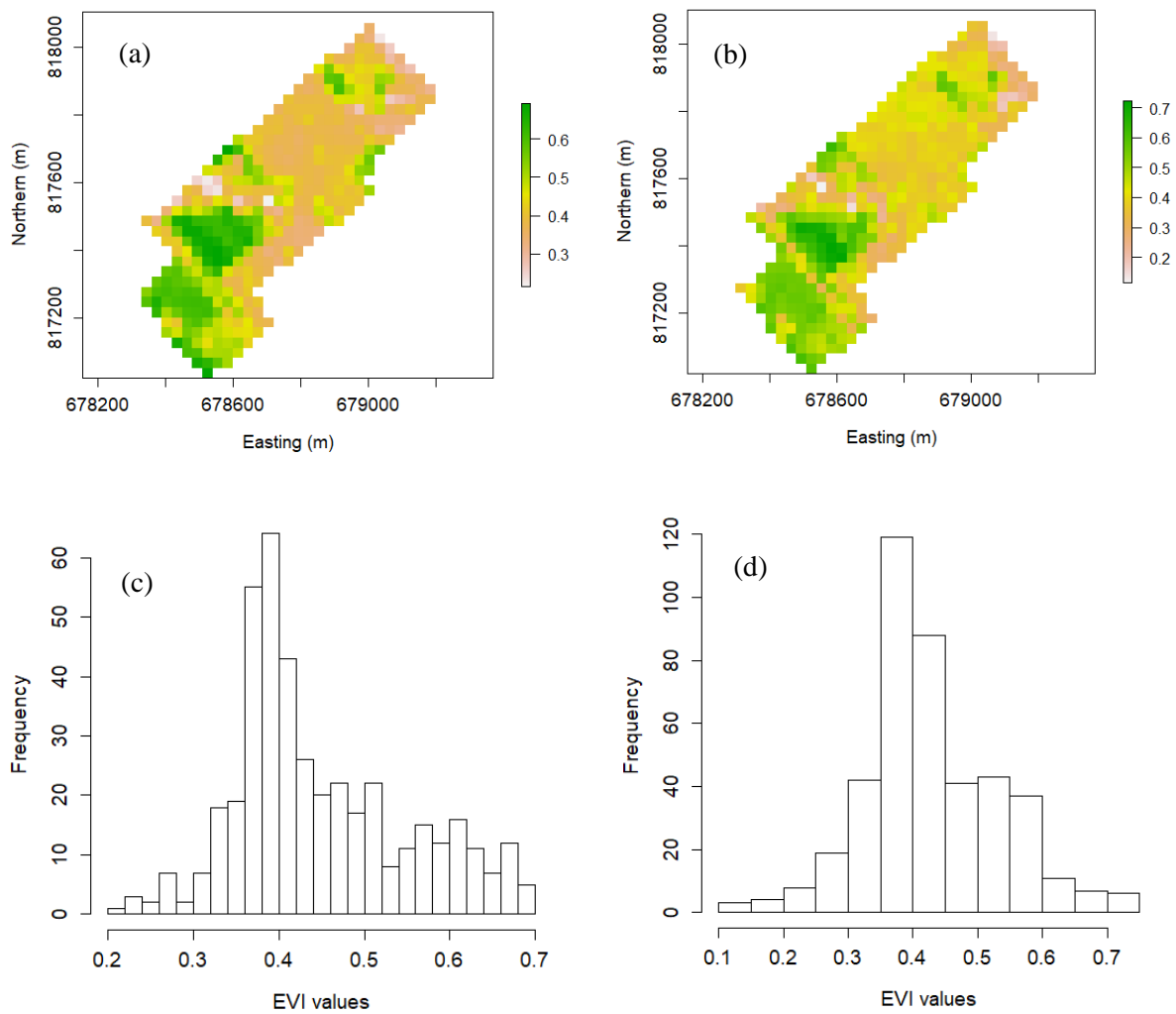


**Figure 3.3:** EVI maps and histogram for Landsat 8 and Parrot Sequoia: (a) Landsat 8 EVI map (b) Parrot Sequoia EVI2 map (c) Landsat 8 EVI histogram (d) Parrot Sequoia EVI2 histogram

Computing the difference (residuals) between EVI from Landsat 8 and EVI2 from Parrot Sequoia gave a mean value of 0.02, with maximum and minimum values of 0.30 and 0.24 respectively. The residuals from the difference between EVI and EVI2 followed a bell-shaped distribution with higher residuals being geographically distributed around the edges and in the south-western section of the study area. Although lower residuals were situated randomly throughout the study area, the central section of the study area registered a larger number of low, negative residuals (see figure 3.4).

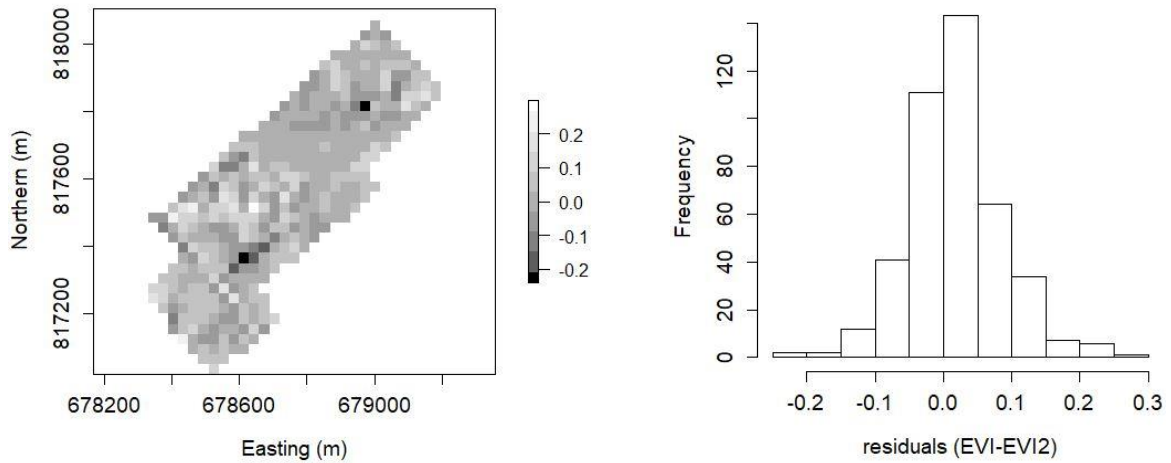


**Figure 3.4:** Map and histogram of EVI-EVI2 residuals respectively

These products were further compared via linear regression to predict EVI from Landsat 8 using EVI2 from Parrot Sequoia. Probability value, intercept and adjusted R-squared from the ordinary least square regression analysis showed positive correlation between EVI and EVI2 (see table 3.1). Plotting predicted values against fitted values from the regression model (figure 3.5) showed that the regression model adopted was acceptable; a symmetrical pattern could be observed around the 0 reference line. interestingly, a cluster of fitted values could be observed around 0.40, -0.04 and 0.45, -0.04.

**Table 3.1:** Results from linear regression analysis

Statistical Quality	Value
Slope	0.76
Intercept	0.12
Probability	2e-16
Adjusted R-squared	0.59

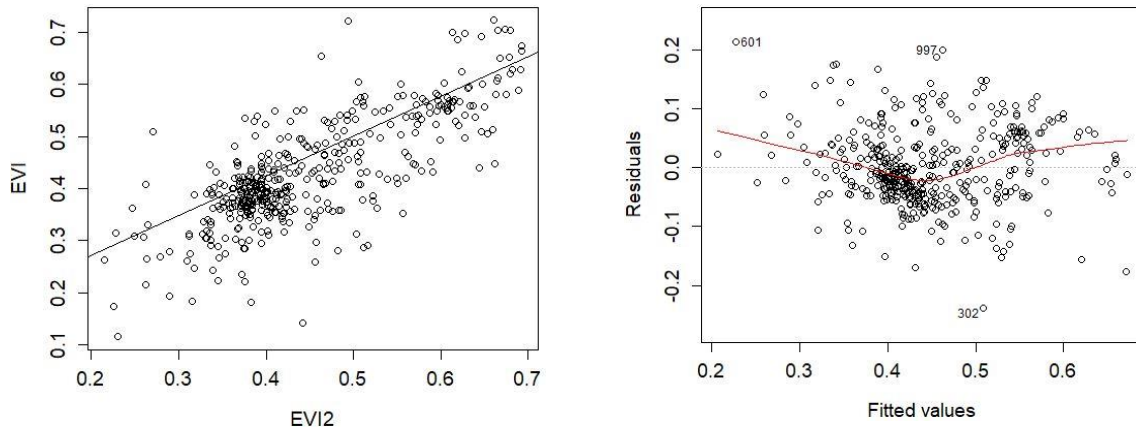


**Figure 3.5:** Scatterplot of EVI and EVI2 as well plot of residuals versus fitted values (left to right respectively)

To validate the robustness of this model, it was used to predict EVI values from a section of the study area that was not included in the initial analysis. Data for the validation site was collected on the same day that the training site was flown and has similar geographical characteristics. Results from the validation process showed a strong positive relationship between observed EVI values and predicted EVI values from Landsat 8 with an adjusted R-squared of 0.61 (figure 3.7). Once again; a map of the residuals (figure 3.6: lower left) depicted lower residuals in areas that were homogeneous in vegetation than areas that had heterogeneous (especially areas with a mixture of dry and green maize foliage) in vegetation. This observed pattern could be due to the time lag between the date of drone image acquisition and Landsat 8 image acquisition.

**Table 3.2:** Results from linear regression analysis on predicted EVI

Statistical Quality	Value
Slope	-0.05
Intercept	1.12
Adjusted R-squared	0.61

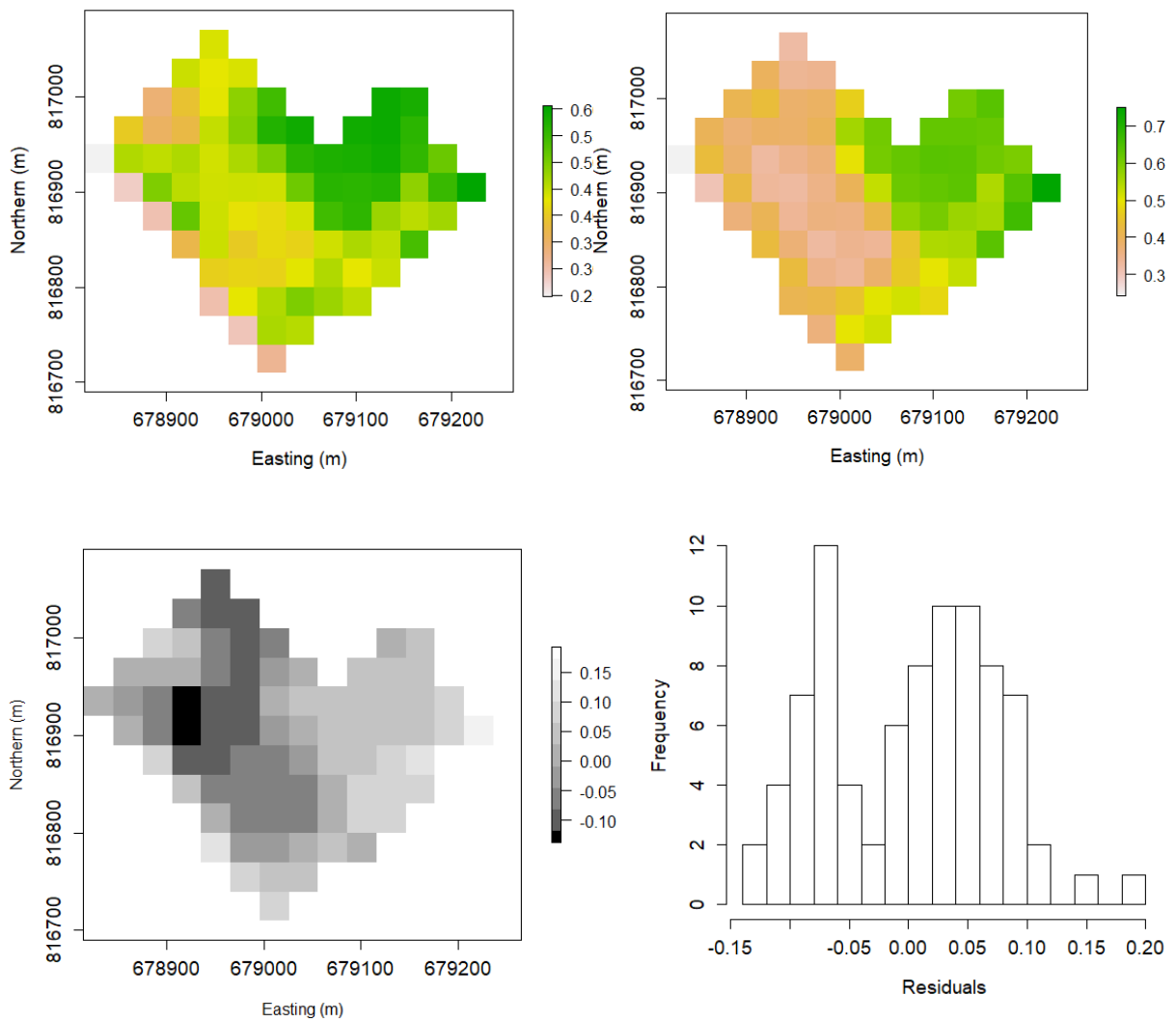


**Figure 3.6:** Predicted EVI map, observed EVI (first row from left to right respectively), difference between observed EVI and predicted EVI maps and histogram (from left to right respectively)

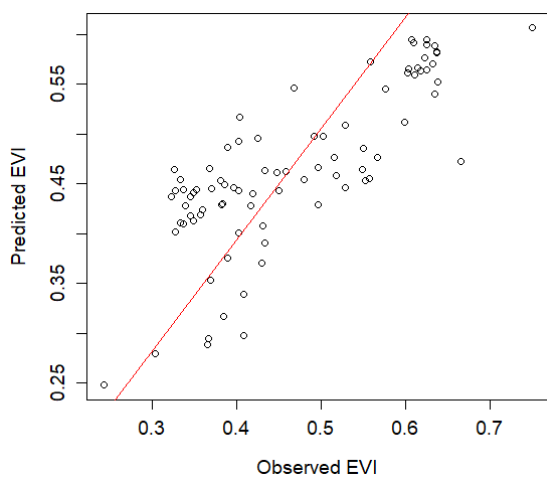


**Figure 3.7:** correlation plot for observed and predicted EVI

### **3.4. Discussion**

Computation of EVI from satellite imagery has been investigated in several studies including (Nagai *et al.*, 2009; Schnur *et al.*, 2010; Setiawan *et al.*, 2014; Son *et al.*, 2014) and continues to be explored by the remote sensing community. However, the difference in the design of UAVs, their high spatial resolution, and their associated multispectral cameras require that a different algorithm be employed in the computation of EVI. Thankfully, Jiang *et al.*, (2008) developed a two band EVI algorithm (EVI2) for low-altitude sensors such as Parrot Sequoia deployed on a UAVs. This work has successfully compared the EVI2 algorithm with EVI computed for high altitude multispectral sensor (Landsat 8) over maize fields in Ejura, Ghana. We initiated the data analysis stage of this work by computing the difference between EVI from Landsat 8 and EVI2 from Parrot Sequoia. Ideally, we would expect the residuals from the difference between EVI and EVI2 to be approximately 0. However, the residuals from the initial analysis had mean, minimum and maximum values of 0.02, -0.24, and 0.299 respectively indicating some differences. The observed difference in residuals could be as a result of the constraints we mentioned at the beginning of this work: (1) difference in sensor band center; (2) impact on data due to spatial resampling techniques; (3) difference in time of image acquisition, since Landsat 8 imagery was acquired four days after acquisition of the Sequoia imagery. However, conscious effort was made to reduce the effect of resampling by using a technique similar to the way Landsat 8 imagery is acquired. The other two constraints therefore play a role in the interpretation of the final results.

### **3.5. Conclusion**

This work has successfully compared EVI developed from Landsat 8 and EVI computed from Parrot Sequoia deployed on a UAV (DJI Phantom4 Pro) by using a novel approach: resampling with the fishnet. While the fishnet technique used for resampling is not

new, it does not appear to have been used to develop imagery from UVA deployed sensors that mimic Landsat 8 resolution for cross-scale comparison. This technique is described in the methods section of this work and remain pivotal to the success of this study. In addition, the EVI2 modeling equation developed here has the potential to predict EVI values that are comparable to Landsat 8 EVI. Results from regression analysis for EVI and EVI2 showed an adjusted R-squared value of 59%, suggesting a relationship between EVI and EVI2 exist. Also using the model developed from the regression analysis for prediction analysis reported a slightly higher adjusted R-squared of 0.61, depicting the robustness of the model developed from the regression analysis.

Given that the study area did not cover a very large geographical region, the reader is encouraged to interpret the results obtained from this work in the context of the study area without extrapolating our findings to area of different geographical settings. Future work in this domain should consider: (1) applying the methodology described in this work to a broader geographical area with high level of contrasting land use; and (2) comparing other vegetation indices such as SAVI from satellite imagery (Sentinel and Landsat 8) with UVA deployed sensors such as Parrot Sequoia and MicaSense RedEdge.

## **CHAPTER 4**

### **CONCLUSIONS**

In this thesis, remote sensing and statistical methods have been used to bridge existing gaps in developing prediction models for African armyworm infestation from imagery and farmer surveys. Findings from this work can be examined in two categories as shown in the second and third chapters. First, a prediction model for the presence or absence of armyworm infestation within the study area (Ejura, Ghana) based on EVI values and slope was developed. The model has the potential of aiding stakeholders in developing detection, early warning, and preventive schemes for African armyworm outbreaks. While results from a logistic regression model showed no correlation between dependent and independent variables, prediction accuracy of 0.61 was recorded from the validation sample. This finding shows the potential of making informed decisions from the model with some improvements such as increasing sample size and including other predictor variables such as precipitation. Results from the second chapter of this work does not necessarily imply abandoning EVI and other vegetation indices as predictors of armyworm infestation (given that this work could not make use of the full EVI spectrum covering the entire maize phenology). This is because several factors could have played a significant role in the results obtained in Chapter two. A potential source of inaccuracy in the EVI values could be the effect of shadows as a results of clouds. While careful efforts were made to reduce the effects of cloud cover within the EVI imagery, the effects of shadows resulting from cloud cover could not be eliminated in this study. It is therefore possible that EVI values that were used for the analysis phase of this work had pixel values corresponding to shadow and not vegetation. Differences in farming practices such as weeding is yet another factor that could have impacted the results of this work. If weed management practices among farmers were very heterogonous then changes in EVI values as result of weed control practices by farmers could have impacted the observation made during the results obtained. There is also

a possibility of EVI not being a robust estimator of armyworm infestation. In this regard exploring other common vegetation indices such as NDVI in combination with EVI could reveal interesting results.

The second part of this work (Chapter 3) has several applications notably: computing EVI for areas that might not have satellite imagery for a given time period, addressing the issue of cloud cover in remote sensing and more specifically satellite imagery at local and regional scales, detecting vegetation health via drone imagery. With respect to the issue of cloud cover, maize phenology for a significant portion of the Ejura region could not be modeled due to the presence of extensive cloud cover in satellite images obtained for this work. This is a general issue when it comes to working with imagery on agricultural regions in the tropics, when the growing season corresponds to times of high cloud cover. To address this issue, imagery from Parrot Sequoia sensor deployed on a UAV was successfully rescaled to match the spectral and spatial information of a Landsat 8 image for the study area. EVI and EVI2 algorithms measure vegetation cover by accounting for aerosols and soil background effects. Needless to say, EVI is usually applied to satellite imagery such as Landsat and MODIS while EVI2 has potential applications in low altitude multispectral sensors such as UAV deployed Parrot Sequoia. A model was developed to predict EVI from EVI2 to assess these differences. The model developed for this purpose performed well in areas with high plant biomass as compared to areas with sparse vegetation. An overall adjusted R-squared of 0.61 showed a strong correlation between Landsat EVI and drone-based resampled EVI2. This finding will, therefore, contribute to existing approaches (such as cloud masking) that have been developed by the remote sensing community to help solve the enigma of cloud cover in remotely sensed data. It is however worth mentioning that comparing vegetation indices or spectral information from different sensors have some challenges. Prominent challenges that specifically applied to this work is difference in spectral, spatial and temporal resolutions. While nothing could be done about the

difference in both spectral and temporal resolution between Landsat 8 and the Parrot Sequoia imagery, the issue of spatial resolution was handled in this work. Resampling Parrot Sequoia imagery to Landsat 8 via a fishnet grid addressed this issue. I therefore admit that the inability of the model developed to predict Landsat 8 EVI with a higher accuracy could be as a result of differences in spectral and temporal resolutions of both sensors.

Collectively, the reader is encouraged to see this work as a contribution to filling the existing gap in applications of remote sensing for combating African armyworm infestations.

## REFERENCES

## REFERENCES

- Abteu, A., Niassy, S., Affognon, H., Subramanian, S., Kreiter, S., Tropea, G., & Martin, T. (2016). Farmers' knowledge and perception of grain legume pests and their management in the Eastern province of Kenya. *Crop Protection*, 87, 90–97. <https://doi.org/10.1016/j.cropro.2016.04.024>
- Acharya, M. C., & Thapa, R. B. (2015). Remote Sensing and its Application in Agriculture Pest Management. *Agriculture and Environment*, 16, 43–61.
- Adama, I., & Mochiah, M. (2017). Assessing the relationship between outbreaks of the African Armyworm and Climatic Factors in the Forest Transition Zone of Ghana. *British Journal of Environment and Climate Change*, 7(2), 69–82. <https://doi.org/10.9734/BJECC/2017/30588>
- Ahmed, O. S., Shemrock, A., Chabot, D., Dillon, C., Wasson, & R., Franklin, S. E. (2017). Hierarchical land cover and vegetation classification using multispectral data acquired from an unmanned aerial vehicle. *International Journal of Remote Sensing*, 38(8–10), 2037–2052. <https://doi.org/10.1080/01431161.2017.1294781>
- Alvarez-Taboada, F., Paredes, C., & Julián-Pelaz, J. (2017). Mapping of the invasive species *Hakea sericea* using Unmanned Aerial Vehicle (UAV) and worldview-2 imagery and an object-oriented approach. *Remote Sensing*, 17. <https://doi.org/10.3390/rs9090913>
- Asiedu, O., Kwoseh, C. K., Melakeberhan, H., & Adjei-Gyapong, T. (2017). Nematode distribution in cultivated and undisturbed soils of Guinea Savannah and Semi-deciduous Forest zones of Ghana. *Geoscience Frontiers*, 1–7. <https://doi.org/10.1016/j.gsf.2017.07.010>
- Baluja, J., Diago, M. P., Balda, P., & Tardaguila, J. (2012). Assessment of vineyard water status variability by thermal and multispectral imagery using an unmanned aerial vehicle (UAV). *Irrigation Science*, 30, 511–522. <https://doi.org/10.1007/s00271-012-0382-9>
- Barlow, V. M., & Kuhar, T. P. (2009). *Fall Armyworm in Vegetable Crops*. Virginia Cooperative Extension (Vol. 444). Virginia.
- Bebber, D. P., Holmes, T., & Gurr, S. J. (2014). The global spread of crop pests and pathogens. *Global Ecology and Biogeography*, 23, 1398–1407. <https://doi.org/10.1111/geb.12214>
- Bobbe, T., Quayle, B., Lannom, K., & Parsons, A. (2001). *Field Measurements for the Training and Validation of Burn Severity Maps from Spaceborne, Remotely Sensed Imagery*. Principal Investigators. Salt Lake.
- Brown, E. S. (2015). Control of the African Armyworm, *Spodoptera exempta* (Walk.)—An Appreciation of the Problem. *East African Agriculture and Forestry*, 35(3), 237–245. <https://doi.org/10.1080/00128325.1970.11662403>
- Caiserman, A., Dumas, D., Bennafla, K., Faour, G., & Amiraslani, F. (2019). Application of

- Remotely Sensed Imagery and Socioeconomic Surveys to Map Crop Choices in the Bekaa Valley ( Lebanon ). *Agriculture*, 19. <https://doi.org/10.3390/agriculture9030057>
- Candiago, S., Remondino, F., Giglio, M. De, Dubbini, M., & Gattelli, M. (2015). Evaluating Multispectral Images and Vegetation Indices for Precision Farming Applications from UAV Images. *Remote Sensing*, (7), 4026–4047. <https://doi.org/10.3390/rs70404026>
- Capinera, J. L. (2017). *Fall Armyworm* , *Spodoptera frugiperda*. Florida.
- Eklundh, L., Johansson, T., & Solberg, S. (2009). Mapping insect defoliation in Scots pine with MODIS time-series data. *Remote Sensing of Environment*, 113(7), 1566–1573. <https://doi.org/10.1016/j.rse.2009.03.008>
- Eze, S. C., & Echezona, B. (2012). Agricultural Pest Control Programmes, Food Security and Safety. *African Journal of Food , Nutrition and Development*, 12(5).
- Faithpraise, F., Idung, J., Chatwin, C., Young, R., & Birch, P. (2015). Modelling the Control of African Armyworm (*Spodoptera exempta*) Infestations in Cereal Crops by Deploying Naturally Beneficial Insects. *Biosystems Engineering*, 20.
- Fang, S., Tang, W., Peng, Y., Gong, Y., Dai, C., & Chai, R. (2016). Remote Estimation of Vegetation Fraction and Flower Fraction in Oilseed Rape with Unmanned Aerial Vehicle Data. *Remote Sensing*, 8(416), 19. <https://doi.org/10.3390/rs8050416>
- Fernández-Guisuraga, J. M., Sanz-Ablanedo, E., Suárez-Seoane, S., & Calvo, L. (2018). Using Unmanned Aerial Vehicles in Postfire Vegetation Survey Campaigns through Large and Heterogeneous Areas: Opportunities and Challenges. *Sensors*, 18(586), 17. <https://doi.org/10.3390/s18020586>
- Garcia-ruiz, F., Sankaran, S., Mari, J., Suk, W., Rasmussen, J., & Ehsani, R. (2013). Comparison of two aerial imaging platforms for identification of Huanglongbing-infected citrus trees. *Computers and Electronics in Agriculture*, 91, 106–115. <https://doi.org/10.1016/j.compag.2012.12.002>
- Ghanaweb. (2017). Army worms attack: 18,200 hectares of maize farm destroyed. Retrieved from <https://www.ghanaweb.com/GhanaHomePage/NewsArchive/Army-worms-attack-18-200-hectares-of-maize-farm-destroyed-542189#>
- Griffiths, P., Nendel, C., & Hostert, P. (2019). Intra-annual reflectance composites from Sentinel-2 and Landsat for national-scale crop and land cover mapping. *Remote Sensing of Environment*, 220, 135–151. <https://doi.org/10.1016/j.rse.2018.10.031>
- Hackney, C., & Clayton, A. I. (2015). Unmanned Aerial Vehicles ( UAVs ) and their application in geomorphic mapping. *Geomorphological Techniques*, 7, 1–12.
- Hijmans, H. J. (2019). raster: Geographic Data Analysis and Modeling. Retrieved from <https://cran.r-project.org/package=raster>
- Holt, J. (2004). *Final Technical Report* (Vol. 7966).
- Honkavaara, E., Saari, H., Kaivosoja, J., Pölönen, I., Hakala, T., Litkey, P., Mäkyne, J., &

- Pesonen, L. (2013). Processing and Assessment of Spectrometric, Stereoscopic Imagery Collected Using a Lightweight UAV Spectral Camera for Precision Agriculture. *Remote Sensing*, 5, 5006–5039. <https://doi.org/10.3390/rs5105006>
- Huete, A., Didan, K., Miura, T., Rodriguez, E. P., Gao, X., & Ferreira, L. G. (2002). Overview of the radiometric and biophysical performance of the MODIS vegetation indices. *Remote Sensing of Environment*, 83, 195–213.
- Idrissa, M., Mbaye N., Sama G., Garba O., & Salissou. O. (2017). *The Fall armyworm Spodoptera frugiperda , the new maize pest in West Africa , has reached Niger. AGRHYMET Regional Centre, SPECIAL Bulletin.*
- Jiang, Z., Huete, A. R., Didan, K., & Miura, T. (2008). Development of a two-band enhanced vegetation index without a blue band. *Remote Sensing of Environment*, 112, 3833–3845. <https://doi.org/10.1016/j.rse.2008.06.006>
- Johnson, S. J. (1987). Migration and the life history strategy of the fall armyworm, *Spodoptera frugiperda* in the western hemisphere. *International Journal of Tropical Insect Science*, 8(4-5-6), 543–549. <https://doi.org/10.1017/S1742758400022591>
- Justice, C. O., Townshend, J. R. G., Holben, B. N., Tucker, C. J., Townshend, J. R. G., Holben, B. N., & Tucker, C. J. (2007). Analysis of the phenology of global vegetation using meteorological satellite data. *International Journal of Remote Sensing*, 6, 1271–1318. <https://doi.org/10.1080/01431168508948281>
- Klemas, V. (2013). Fisheries applications of remote sensing: An overview. *Fisheries Research*, 148, 124–136. <https://doi.org/10.1016/j.fishres.2012.02.027>
- Lausch, A., Heurich, M., Gordalla, D., Dobner, H. J., Gwilym-Margianto, S., & Salbach, C. (2013). Forecasting potential bark beetle outbreaks based on spruce forest vitality using hyperspectral remote-sensing techniques at different scales. *Forest Ecology and Management*, 308, 76–89. <https://doi.org/10.1016/j.foreco.2013.07.043>
- Lelong, C. C. D., Burger, P., Jubelin, G., Roux, B., Labbé, S., & Baret, F. (2008). Assessment of Unmanned Aerial Vehicles Imagery for Quantitative Monitoring of Wheat Crop in Small Plots. *Sensors*, 8, 3557–3585. <https://doi.org/10.3390/s8053557>
- Matsushita, B., Yang, W., Chen, J., Onda, Y., & Qiu, G. (2007). Sensitivity of the Enhanced Vegetation Index (EVI) and Normalized Difference Vegetation Index (NDVI) to topographic effects: A case study in high-density cypress forest. *Sensors*, 7, 2636–2651. <https://doi.org/10.3390/s7112636>
- Melesse, A. M., Weng, Q., Thenkabail, P. S., & Senay, G. B. (2007). Remote Sensing Sensors and Applications in Environmental Resources Mapping and Modelling. *Sensors*, 7, 3209–3241.
- Midega, C. A. O., Nyang, I. M., Pittchar, J., Birkett, M. A., Pickett, J. A., Borges, M., & Khan, Z. R. (2012). Farmers' perceptions of cotton pests and their management in western Kenya. *Crop Protection*, 42, 193–201. <https://doi.org/10.1016/j.cropro.2012.07.010>
- Miller, R. B., & Small, C. (2003). Cities from space : potential applications of remote sensing

- in urban environmental research and policy. *Environmental Science and Policy*, 6, 129–137. [https://doi.org/10.1016/S1462-9011\(03\)00002-9](https://doi.org/10.1016/S1462-9011(03)00002-9)
- Miyazaki, H., Iwao, K., & Shibasaki, R. (2011). Development of a New Ground Truth Database for Global Urban Area Mapping from a Gazetteer. *Remote Sensing*, 3, 1177–1187. <https://doi.org/10.3390/rs3061177>
- Mogili, U. M. R., & Deepak, B. B. V. L. (2018). ScienceDirect ScienceDirect Review on Application of Drone Systems in Precision Agriculture. *Procedia Computer Science*, 133, 502–509. <https://doi.org/10.1016/j.procs.2018.07.063>
- Montandon, L. M., & Small, E. E. (2008). The impact of soil reflectance on the quantification of the green vegetation fraction from NDVI. *Remote Sensing of Environment*, 112, 1835–1845. <https://doi.org/10.1016/j.rse.2007.09.007>
- Morton. (2013). *Population and Housing Census: Ejura sekyedumasi municipal*.
- Nagai, S., Saigusa, N., Muraoka, H., & Nasahara, K. N. (2009). What makes the satellite-based EVI – GPP relationship unclear in a deciduous broad-leaved forest? *The Ecological Society of Japan*, 25, 359–365. <https://doi.org/10.1007/s11284-009-0663-9>
- Nboyine, J. A., Kusi, F., & Adu, G. B. (2017). *Fall Armyworm Outbreak in Ghana – Facts and Management Approaches*. Kumasi. <https://doi.org/10.13140/RG.2.2.33992.52481>
- Nespeca, R., Vaillancourt, J., & Morrow, W. E. M. (1997). Validation of a poultry biosecurity survey. *Preventive Veterinary Medicine*, 31, 73–86.
- Peng, D., Wu, C., Li, C., Zhang, X., Liu, Z., Ye, H., Luo, S., Liu, X., Hu, Y., & Fang, B. (2017). Spring green-up phenology products derived from MODIS NDVI and EVI: Intercomparison, interpretation and validation using National Phenology Network and AmeriFlux observations. *Ecological Indicators*, 77, 323–336. <https://doi.org/10.1016/j.ecolind.2017.02.024>
- Pisani, A. L., Goroza, G., Kabira, J. G., Laing, M. V., Lekhal, R., Lukando, M. F., Makarau, A., & Mersha, E. (2000). *Report on the RA I working Group On Agriculture and Meteorology*. Geneva.
- Prabhakar, M., Prasad, Y. G., Vennila, S., Thirupathi, M., Sreedevi, G., Ramachandra Rao, G., & Venkateswarlu, B. (2013). Hyperspectral indices for assessing damage by the solenopsis mealybug (Hemiptera: Pseudococcidae) in cotton. *Computers and Electronics in Agriculture*, 97, 61–70. <https://doi.org/10.1016/j.compag.2013.07.004>
- Rai, M., & Ingle, A. (2012). Role of nanotechnology in agriculture with special reference to management of insect pests. *Applied Microbiol Biotechnology*, 94, 287–293. <https://doi.org/10.1007/s00253-012-3969-4>
- Rajitha, K., Mukherjee, C. K., & Chandran, R. V. (2007). Applications of remote sensing and GIS for sustainable management of shrimp culture in India. *Aquacultural Engineering*, 36, 1–17. <https://doi.org/10.1016/j.aquaeng.2006.05.003>
- Riley, J. R. (1989). Remote Sensing in Entomology. *Annual Review of Entomology*, 34, 247–

2471.

- Rocha, A. V., & Shaver, G. R. (2009). Agricultural and Forest Meteorology Advantages of a two band EVI calculated from solar and photosynthetically active radiation fluxes. *Agricultural and Forest Meteorology*, *149*, 1560–1563. <https://doi.org/10.1016/j.agrformet.2009.03.016>
- Roosjen, P. P. J., Brede, B., Suomalainen, J. M., Bartholomeus, H. M., Kooistra, L., & Clevers, J. G. P. W. (2018). Improved estimation of leaf area index and leaf chlorophyll content of a potato crop using multi-angle spectral data – potential of unmanned aerial vehicle imagery. *International Journal of Applied Earth Obs Geoinformation*, *66*, 14–26. <https://doi.org/10.1016/j.jag.2017.10.012>
- Rose, D. J. W., Dewhurst, C. F., Page, W. W., & Fishpool, L. D. C. (1987). The Role of Migration in the Life System of the African Armyworm. *Applied Insect Science*, *8*, 561–569.
- Schnur, M. T., Xie, H., & Wang, X. (2010). Ecological Informatics Estimating root zone soil moisture at distant sites using MODIS NDVI and EVI in a semi-arid region of southwestern USA. *Ecological Informatics*, *5*, 400–409. <https://doi.org/10.1016/j.ecoinf.2010.05.001>
- Setiawan, Y., Yoshino, K., & Budi, L. (2014). Characterizing the dynamics change of vegetation cover on tropical forestlands using 250 m multi-temporal MODIS EVI. *International Journal of Applied Earth Observations and Geoinformation*, *26*, 132–144. <https://doi.org/10.1016/j.jag.2013.06.008>
- Sibanda, D. Z. (2004). *Training Manual on Fall Armyworm. Development*.
- Son, N. T., Chen, C. F., Chen, C. R., Minh, V. Q., & Trung, N. H. (2014). A comparative analysis of multitemporal MODIS EVI and NDVI data for large-scale rice yield estimation. *Agricultural and Forest Meteorology*, *197*, 52–64. <https://doi.org/10.1016/j.agrformet.2014.06.007>
- Stöcker, C., Bennett, R., Nex, F., Gerke, M., & Zevenbergen, J. (2017). Review of the Current State of UAV Regulations. *Remote Sensing*, *26*. <https://doi.org/10.3390/rs9050459>
- Team, R. core. (2017). R: A language and environment for statistical computing. R Foundation for Statistical Computing. Vienna,. Retrieved from <https://www.r-project.org/>
- Tessier, S. (2012). From Field Notes , to Transcripts , to Tape Recordings : Evolution or Combination? *International Journal of Qauntitative Methods*, *11*(4), 446–460. <https://doi.org/10.1177/160940691201100410>
- Testa, S., Soudani, K., Boschetti, L., & Mondino, E. B. (2018). MODIS-derived EVI , NDVI and WDRVI time series to estimate phenological metrics in French deciduous forests. *International Journal of Applied Earth Observation Geoinformation*, *64*, 132–144. <https://doi.org/10.1016/j.jag.2017.08.006>
- Torres-Sánchez, J., Peña, J. M., Castro, A. I. De, & López-Granados, F. (2014). Multi-temporal

- mapping of the vegetation fraction in early-season wheat fields using images from UAV. *Computers and Electronics in Agriculture*, 103, 104–113. <https://doi.org/10.1016/j.compag.2014.02.009>
- Torresan, C., Berton, A., Carotenuto, F., Di, S. F., Gioli, B., Matese, A., Miglietta, F., Zaldei, A., & Wallace, L. (2017). Forestry applications of UAVs in Europe : a review Forestry applications of UAVs in Europe : a review. *International Journal of Remote Sensing*, 38(8–10), 2427–2447. <https://doi.org/10.1080/01431161.2016.1252477>
- Turner, W., Spector, S., Gardiner, N., Fladeland, M., Sterling, E., & Steininger, M. (2003). Remote sensing for biodiversity science and conservation. *Trends in Ecology and Evolution*, 18(6), 306–314. [https://doi.org/10.1016/S0169-5347\(03\)00070-3](https://doi.org/10.1016/S0169-5347(03)00070-3)
- Vidich, A., & Bensman, J. (1954). The Validity of Filed Data. *Human Organization*, 13(1), 20–27.
- Wilson, K., & Gatehouse, A. G. (1992). Migration and genetics of pre-reproductive period in the moth , *Spodoptera exempta* ( African armyworm ). *Heridity*, 69(September 1992). <https://doi.org/10.1038/hdy.1992.123>
- Wulder, M. A., Masek, G. J., Cohen, W. B., Loveland R., T., & Woodcock, C. E. (2012). Opening the archive : How free data has enabled the science and monitoring promise of Landsat. *Remote Sensing of Environment*, 122, 9.
- Xiang, H., & Tian, L. (2011). Development of a low-cost agricultural remote sensing system based on an autonomous unmanned aerial vehicle ( UAV ). *Biosystems Engineering*, 108, 174–190. <https://doi.org/10.1016/j.biosystemseng.2010.11.010>
- Xiao, X., Braswell, B., Zhang, Q., Boles, S., Frohling, S., & Iii, B. M. (2003). Sensitivity of vegetation indices to atmospheric aerosols : continental-scale observations in Northern Asia. *Remote Sensing of Environment*, 84, 385–392.
- Yang, Z., Rao, M. N., Elliott, N. C., Kindler, S. D., & Popham, T. W. (2009). Differentiating stress induced by greenbugs and Russian wheat aphids in wheat using remote sensing. *Computers and Electronics in Agriculture*, 67(1–2), 64–70. <https://doi.org/10.1016/j.compag.2009.03.003>
- Zhu, S., Zhang, H., Liu, R., Cao, Y., & Zhang, G. (2014). Comparison of Sampling Designs for Estimating Deforestation from Landsat TM and MODIS Imagery : A Case Study in Mato Grosso , Brazil. *The Scientific World Journal*, 10.
- Zhu, Z., & Woodcock, C. E. (2012). Object-based cloud and cloud shadow detection in Landsat imagery. *Remote Sensing of Environment*, 118, 83–94. <https://doi.org/10.1016/j.rse.2011.10.028>